Combustion of NH_4ClO_4-Polyurethane Propellants: Pressure, Temperature, and Gas-Phase Composition Fluctuations

J. L. EISEL*
Naval Weapons Center, China Lake, Calif.
AND
N. W. RYAN† AND A. D. BAER†
University of Utah, Salt Lake City, Utah

The spectral and temporal details of the flames of a series of NH_4C10_4-polyurethane propellants during both unstable and stable combustion were observed experimentally. A 400 scan/sec optical spectrometer operating in the middle infrared region was used to follow the concentrations and temperature of the combustion procducts. Both bulk mode instability and intrinsic instability were observed separately and, under some conditions, coupled. Some aspects of the theory of bulk mode instability were confirmed but the assumptions of constant flame temperature and constant composition were found to be inaccurate. Observed fluctuations in temperature of up to 500°C and in composition of up to 40% were explained by the assumption of a fluctuating surface composition and gas phase quasi-equilibrium resulting in composition waves in the combustion chamber. These phenomena were strongly influenced by the propellant heterogeneity.

Nomenclature

C_1 = constant in Planck's Law; 3.74×10^{-12} w cm^2
C_2 = constant in Planck's Law; 1.438 cm °K
C_D = nozzle discharge coefficient; sec/cm
D_i = nominal diameter of ith AP particle-size fraction; cm
I = intensity of radiation; w/cm^2 steradian μm
K_i = proportionality factor between layer frequency due to the ith AP particle-size fraction and r/D_i
L^* = characteristic length (chamber free volume/nozzle throat area); cm
P = total chamber pressure; psia
p = partial pressure; psi
R = universal gas constant; (cal/g mole °K)
r = burning rate; cm/sec
T = temperature; °K
X_i = fraction of total propellant weight due to ith AP particle-size
α = exponential growth constant of oscillatory pressure from $P = \bar{P} + P_0 e^{\alpha t} \cos \omega t$; sec^{-1}
λ = wavelength; μm
ω = angular frequency; rad/sec
$\omega\tau$ = phase lead of mass efflux rate with respect to pressure; rad
μ = molecular weight; g/g mole
ρ = density; g/cm^3

Subscripts

A = absorption
E = emission
g = gas phase
f = fuel
N = value to which normalized
0 = initial value or intercept value
ox = oxidizer
P = value normalized to a fixed pressure, P_N
s = due to radiation source
T = value normalized to a fixed temperature, T_N

Presented as Paper 72-32 at the AIAA 10th Aerospace Sciences Meeting, San Diego, Calif., January 17–19, 1972; submitted March 6, 1972; revision received August 3, 1972. This research was supported by NASA Grant NGL 45-003-019 and Naval Weapons Center Fellowship.

Index categories: Combustion Stability, Ignition, and Detonation; Combustion in Heterogeneous Media.

* Research Engineer, Aerothermochemistry Division, Naval Weapons Center, China Lake, Calif.

† Professor of Chemical Engineering. Associate Fellow AIAA.

Introduction

THE instantaneous thermochemical environment which exists in a rocket motor during unstable combustion is extremely complicated. Although the contributions to the theoretical and experimental understanding of unstable combustion of solid propellants have been legion, this area of thermochemical environment has been ignored almost totally. The present work experimentally elucidates some of the chemical variations which occur in the propellant flame above the burning surface. Although the complete analysis of the chemical environment was not possible, it was possible to follow the major species as their concentrations varied in time during unstable combustion. From these measurements the relative flame temperature and the phase relationships between the pressure, temperature and composition fluctuations were calculated. These measured and calculated values provide the basis for a discussion of the possible mechanisms involved.

The observations were made using a rapid-scanning optical spectrometer operating in the middle infrared spectral region (1.7 μm to 4.8 μm). As low L^*, or bulk mode (BMI), instability[1-4] is most easily amenable to theoretical analysis and because this phenomenon can be caused to occur at low frequencies and low pressures, this was the process chosen for observation. The propellants whose flames were observed were 80/20 mixtures of NH_4ClO_4(AP) and estane-based polyurethane. They were tailored to be unstable at relatively large values of L^* (up to 250 cm) and at low pressure (below 60 psia) and at low frequency (10 to 100 Hz).

Theoretical descriptions of unstable combustion have been based upon simplifying assumption.[5,6] Usually, a one-dimensional, linear analysis is performed,[5] although exceptions exist.[7,8] Such assumptions as constant flame temperature, quasi-steady gas phase conditions, homogeneous solid phase, and burning rates determined by initial temperature and chamber pressure only[5] are also made. Further, and related directly to these other assumptions, it is universally assumed, if not actually believed, that the composition is spatially and temporally uniform (see Ref. 6 for a good discussion). Fluctuations in flame temperature during instability have been previously reported[9] and the effects of temperature on L^* instability discussed theoretically.[10]

Experimental Setup

The experimental aspects of the present study were centered about a rapid scanning infrared spectrometer (as an observational

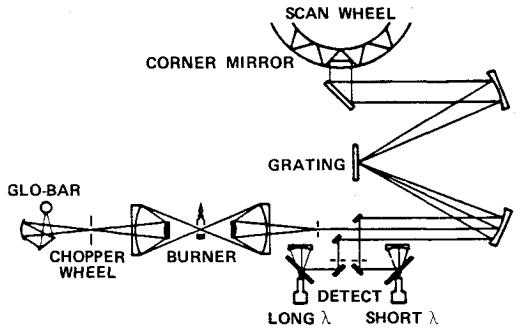

Fig. 1 Schematic layout of spectroscopic system showing dual wavelength output.

tool) and a test device (either a solid rocket propellant burner or the shock tube used in preliminary studies).

The spectrometer (Warner and Swasey, Control Instrument Division, Model 501) was a rapid scanning device (Fig. 1) capable of scanning rates of from 8 scan/sec up to 800 scans/sec. As used throughout the present study, it was operated in the 1.7 μm to 4.8 μm wavelength range and at 1.0 millisecond per scan. Entrance and exit slits were set at 0.5 mm.

In addition to the spectrometer, there was a radiation source unit in which a silicon carbide Globar was located which could be controlled to within 4°C at temperatures from 1000°C to 1225°C. This radiation was focused on the test section by a Cassegrain system matched to an identical unit in the entrance section of the receiver and provided a means for doing absorption spectroscopy. Further, this external radiation source beam was interrupted periodically in synchronization with the scanning of the receiver to provide alternate emission and emission-absorption information from the test phenomenon. This procedure reduced the time resolution by a factor of two, but provided a means for measuring temperature.

The outputs from the two solid state (InAs and InSb) detectors were pre-amplified and displayed on the face of a dual beam oscilloscope in a vertical deflection mode (no time base). In addition, the output from a pressure transducer (Kistler 601L) was displayed in a chopped mode on the same channel as the short wavelength detector output. This total display was then photographed during a test by a horizontally mounted Fastax streak camera which provided the time dimension for the displayed data. An absolute time calibration was unnecessary since, during the 1.25 msec of scan the rate of change of the time-base was negligible. The spectral scans were provided with timing marks which served as calibrated end points of the linear wavelength display.

Design of the Burner-Propellant System

As discussed earlier, the aim of the present program was the spectral observation of the unstable burning of solid rocket propellants. The success of such an undertaking was dependent upon several interlocking considerations. These centered about the design of a burner and a series of propellants which would produce the low pressure, low-frequency behavior desired in a manner amenable to observation by the optical spectrometer.

The physical setup placed several constraints on the solution to these design problems. First, since the spectrometer had a scan repetition time of 1.25 msec, it was necessary to produce an instability with a period no shorter than eight to ten times the scan time, that is, 125 to 100 Hz when the system was run in an emission only mode or about 62 to 50 Hz when emission-absorption measurements were made. The latter was the mode employed and, as will be noted later, this limit was exceeded during part of the experiment. Further, in order that the physical size limitations of the burner interior would not obstruct the view through the flame and also that chemical species produced at the outside edge of the burning diameter would not be in the field of view longer than the time needed to cross the view path at right angles to its direction, it was necessary to design a propellant which was unstable at relatively large values of L^*; that is, where a relatively large free volume was present during the unstable combustion. Finally, there was an obvious need for a "clean burning" propellant, i.e., one which did not produce continuum radiation.

Table 1 Comparison between calculated and observed layer frequencies

Desig.	Propellant Composition	Frequency Calculated	Frequency Observed
UCD	0.20 estane + curative		
	0.55 AP (600 μm)	3.3 Hz	2–3 Hz
	0.25 AP (90 μm)	9.9 Hz	10–15 Hz
UDO	0.20 estane + curative		
	0.55 AP (600 μm)	3.3 Hz	2–3 Hz
	0.25 AP (70 μm)	12.59 Hz	16–20 Hz
UDN	0.20 estane + curative		
	0.55 AP (600 μm)	3.1 Hz	2–3 Hz
	0.25 AP (50 μm)	16.56 Hz	40–50 Hz
UCT	0.20 estane + curative		
	0.55 AP (600 μm)	2.9 Hz	2–3 Hz
	0.25 AP (15 μm)	51.5 Hz	70–80 Hz

A review of the literature[1-4] indicated that the majority of the BMI research carried out in the past was done for propellants which were unstable at frequencies too high and at L^* values too low to be useful in the present program. This necessitated the design of a new series of propellants.

The first aspect of propellant design was the choice of a fuel which, when burned with AP produced a relatively continuum-free radiation signature. From past personal experience and the work of Schulz[11] it was clear that of the fuels available a polyurethane binder was most appropriate. In addition, although many propellants contain burning rate catalysts or darkening agents to limit radiant energy penetration, the desire for a clean flame precluded their incorporation.

A universal trend reported by laboratories investigating L^* instability is that critical L^* (stability limit) increases with decreasing burning rate (or pressure). Therefore, the choice of polyurethane as a fuel was doubly desirable since, in general, polyurethane propellants have lower burning rates than comparable propellants employing other fuel ingredients. The use of large oxidizer particles is well known to lower the burning rate of a propellant of fixed fuel to oxidizer ratio. The Naval Weapons Center (NWC), China Lake, California, supplied AP of 600 μm nominal diameter.

Although present theories of BMI do not allow for the effect of particle size on the frequency of the instability of a system

Table 2 Burning rates of propellants at selected pressures over the range of the experiment from smoothed data

Propellant	P, atm	r_b, cm/sec
UCD	2	0.16
	3	0.19
	4	0.23
UDO	2	0.16
	3	0.19
	4	0.22
UDN	2	0.13
	3	0.18
	4	0.22
UCT	2	0.13
	3	0.15
	4	0.18

except as it affects the burning rate, it has been shown[12] that particle sizes can affect the frequency. Therefore, a series of propellants was formulated with identical chemical composition, but with a variation of the nominal diameter of a portion of the AP amounting to 25%, by weight, of the propellant. The propellant designed, then, was 20% polyurethane plus curing agent, 55% 600 μm AP and 25% AP varying from 90 μm to 15 μm depending on the frequency desired. The burning rate was dominated by the large AP particles and the frequency by the small AP particles. A summary of the formulations used is included in Table 1. Burning rates at selected pressures over the range of the experiment are given in Table 2.

The L^* burner, as it has most often been used,[2] does not meet the criteria for the present work, set forth above, in several respects. The volume is generally small due, not to the burner, but to the propellants usually tested. However, since a need for only a moderate increase in free volume was achieved by the propellant design, a means for removing combustion products without flow parallel to the field of view was necessary. In addition a means of maintaining clean viewing ports was needed. Figure 2 shows two versions of the modified L^* burner used in the present study. When the allowable free volume was large, the burner with the streamlined entrance section was used. Where a smaller free volume was needed the burner utilizing the nineteen-nozzled end wall was used in order to remove combustion products in a manner which minimized transverse gas flow. The early L^* burners generally made use of fixed length interchangeable burner bodies. The present burner, in both of its variations, is provided with an infinitely variable, threaded section (see Fig. 2a) which is calibrated and which provides reduced hardware needs and continuous variation of free volume.

Windows were installed on opposite sides of the burner to allow both viewing of emitted radiation and viewing of radiation from the source unit focused from the opposite side of the burner and transmitted through the combustion chamber. The spectrometer optics were uncollimated so that spatial resolution was minimal. Observations were made about 0.5 cm above the regressing surface, but averaged over a wedge of radiating gases which expanded at about 12° included angle. The window material used exclusively was 3.17-mm-thick sapphire. The transmissivity of the window sapphire as a function of wavelength was determined experimentally over the wavelength range of the infrared detection system. At the long wavelength limit of 4.8 μm the transmissivity drops rapidly. For radiation measurements at longer wavelengths other window materials would be necessary, thus forsaking the exceptional physical properties of sapphire. In addition to high transmissivity windows it was necessary to provide a means of keeping the products of combustion (or partial combustion near the edge of the burner) from condensing upon the window surface and thereby obscuring the view of the flame and of the external radiation source. A gas flushing system was provided whereby gas at relatively high pressure could be introduced into a manifold within the burner from which it flowed from an orifice on the upstream side of each window and out into the combustion chamber. The gas used was air from which the CO_2 and H_2O had been removed. It was added at an oxygen addition rate equivalent to about 6% of the oxygen available from the propellant. Experimentally it was shown that the windows, when an air purge was used, remained almost fog-free whereas when nitrogen was used, although the viewing was an improvement over no purging, a haze of considerable density was deposited. It is assumed that the incompletely oxidized combustion products approaching the window were hot enough to react to completion with the incoming cold air.

Identification of Spectral Details of Combustion

Figure 3 is a typical record of the spectrum of a burning polyurethane and AP propellant. The spectral range is from 1.7 μm to 4.8 μm. The figure includes a pressure trace which is relatively constant during the time interval of $2\frac{1}{2}$ msec shown. The various peaks which can be identified[13] are indicated in the figure. They include CO_2 bands at about 4.3 μm and 2.7 μm. These correspond to the ν_3 parallel antisymmetric stretching mode and a combination of the $\nu_1 + \nu_3$ parallel antisymmetric stretching and first overtone of the parallel bending mode respectively (see Ref. 13, page 66). They also include H_2O bands at nominally 3.2 μm, 2.7 μm, 2.5 μm, 1.9 μm and 1.7 μm. (Also included is an apparent peak at the overlap of the 3.2 μm peak and the edge of the short wavelength detector sensitivity at about 2.9 μm.) These correspond to the $2\nu_2$ first harmonic of the parallel bending mode, the ν_1 symmetric stretching mode, ν_3 antisymmetric stretching mode, $\nu_2 + \nu_3$ combination of the fundamental bending and antisymmetric stretching modes, and $2\nu_2 + \nu_3$ combination of first harmonic of the bending mode and antisymmetric stretching mode, respectively. The frequency of this latter, $2\nu_2 + \nu_3$, vibration had an apparent shift from its 1.45 μm value due to a cutoff of the detector at a longer wavelength than the real peak similar to the problem noted for the $2\nu_2$ vibration. In addition the fundamental stretching band of HCl appears at about 3.5 μm, but extends from less than 3.3 μm to greater than 3.8 μm (see Ref. 13, page 55). And, finally, the fundamental and first harmonic CO bands at 4.6 μm and 2.3 μm, respectively, may be seen.

The other major constituents of the gaseous flame are H_2 and N_2 but, because of their symmetry and charge balance, do not exhibit a net change in dipole moment during their vibrations and therefore emit no IR radiation.

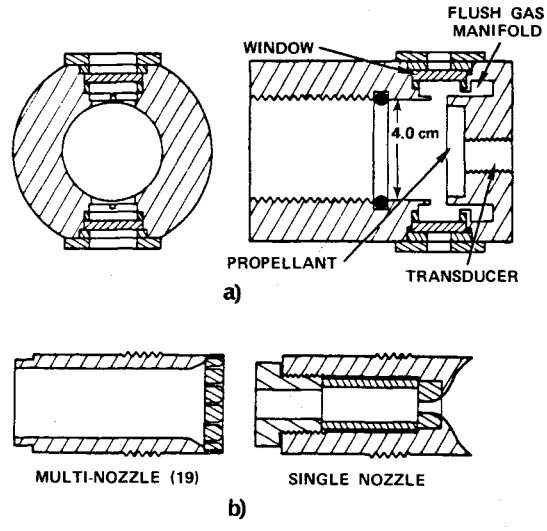

Fig. 2 a) L^* burner used in present study with flushed viewing ports and variable volume; b) two options of nozzle and retainer system used. Single nozzle with streamlined entrance for large L^* tests and nineteen-nozzled flat end for small L^* tests.

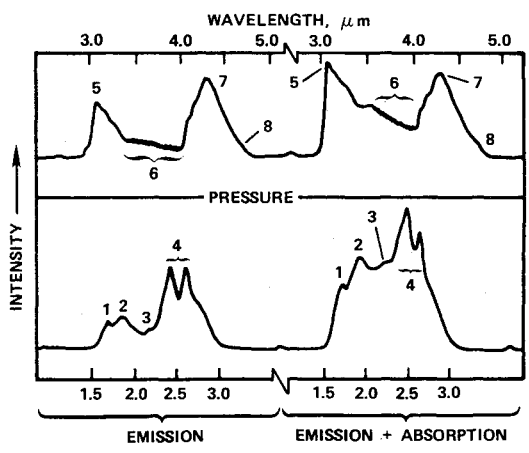

Fig. 3 A typical spectrum of a polyurethane-AP propellant flame. Peaks are identified as follows: 1, 2, 4, 5, H_2O; 4 and 7 CO_2; 6, HCl; and 3 and 8, CO (details in text); pressure is essentially constant during the scan time.

The bands that were followed in this study were the 4.3 μm CO_2, 1.9 μm H_2O, and 4.6 μm CO. The rationale for using the 4.3 μm CO_2 band and the 1.9 μm H_2O band exclusively in the combustion studies has to do with the degree of overlapping of bands. In the 2.5 to 2.7 μm region, although the amplitude is large, the three H_2O peaks are badly overlapped by the one CO_2 band. Ferriso and Ludwig[14] made a study of the H_2O + CO_2 bands in this region. As can be seen in that work the resultant spectral structure in that region is a quite complicated function of relative partial pressures, total pressure, and temperature. The 1.7 μm, 1.9 μm and 3.2 μm bands of H_2O are all quite isolated. However, both the 3.2 μm and 1.7 μm bands, as pointed out earlier, are the edges of bands which peak outside the spectral range of the detectors used. Therefore, by elimination, the 1.9 μm H_2O band and the 4.3 μm CO_2 band were chosen.

The observation of CO was more difficult. The bands at 4.6 μm and 2.3 μm were both of low intensity and badly overlapped by strong adjacent bands. Rather arbitrarily the 4.6 μm peak was chosen in spite of the difficulty in measurement and the extreme overlapping. For these reasons the CO data must not be given too much credence.

Hydrogen chloride exhibits a rather broad band of very distinct rotational fine structure. Its vibrational amplitude, however, is fairly small making more than the most qualitative assessment of intensity almost impossible.

Equilibrium Combustion Calculations

Preliminary information regarding the expected combustion product compositions, mole fractions, and temperatures in the range of the tests to be conducted was obtained using a thermochemical equilibrium computer program.‡ This program, although capable of more extensive calculations, was used to calculate combustion chamber conditions of composition and temperature for input chamber pressure, exit pressure, propellant composition and heat of formation for each constituent.§ Figures 4 and 5 exhibit the results of these calculations. It should be noted that, for equilibrium combustion, at fixed propellant composition, there is no composition variation as a function of pressure over a range wider than that of the experimental program. The temperature does not vary more than 50°C over the pressure range of the program. On the other hand, when pressure is maintained constant and the composition of the propellant being burned is varied, it can be seen that a fairly severe variation in composition of the combustion products results. In particular, the temperature varies significantly—almost 500°K—over the range plotted and the slope of the temperature curve also has the same sign as that of the H_2O and CO_2 curves. Also note that the CO_2 mole fraction varies by about 50% over the whole range.

Data Reduction

The emission spectra of hot gases are dependent on a number of parameters such as pressure, temperature, optical path length and flame density. For these spectra to be useful as gages of the composition of the particular gas mixture during transient conditions it is necessary to adjust the measured peak height values to their expected values at some arbitrary, fixed set of conditions. Once done, any fluctuations in the normalized intensities then represent fluctuations in the composition of the gas mixture being observed.

In the present study the optical path length was fixed at a value identical to that which existed during the shock tube calibration work[15] and the normalizing temperature and pressure were taken to be 2600°K and 30 psia, respectively.

Temperature effects were adjusted based on two major assumptions: ideal gas and Planck's law. Since the ideal gas law predicts that as temperature increases with constant pressure and volume the concentration will decrease, fewer radiators are present, and hence, lower intensity. Moreover, Planck's law predicts that those radiators that are present will emit higher intensities. The result is that the temperature adjustment is not severe, owing to the compensating effects noted. Thus, the temperature adjustment applied was the following:

$$I_T = I \frac{T}{T_N} \frac{\exp(C_2/\lambda T) - 1}{\exp(C_2/\lambda T_N) - 1} \tag{1}$$

The adjustment for pressure fluctuation is more critical and hence more open to criticism. As the pressure increases the ideal gas assumption (which is quite good in spite of somewhat elevated pressure because of the very high temperature) predicts an increased number of radiators and therefore a more intense radiation. The critical point comes when one attempts to relate intensity to concentration. If one simply assumes that the ideal gas law $C = P/RT$ can be replaced by $I = P/RT$ the adjusted intensity becomes

$$I_P = IP_N/P \tag{2}$$

Such an assumption is based on a linear relationship between I and P with no intercept. However, such an assumption does not fit the experimental I vs P relationship and leads to a physically unrealistic situation in which the fluctuations in intensity, and therefore in composition, vary in a way exactly opposite to that predicted by equilibrium calculations. That is, as the pressure increases and the temperature increases the concentrations of both H_2O and CO_2 decrease. The error in such an approach lies in the assumption that concentration is directly replaceable by intensity in the ideal gas law. The correct relationship is

$$I_P = I[I(P_N)/I(P)] \tag{3}$$

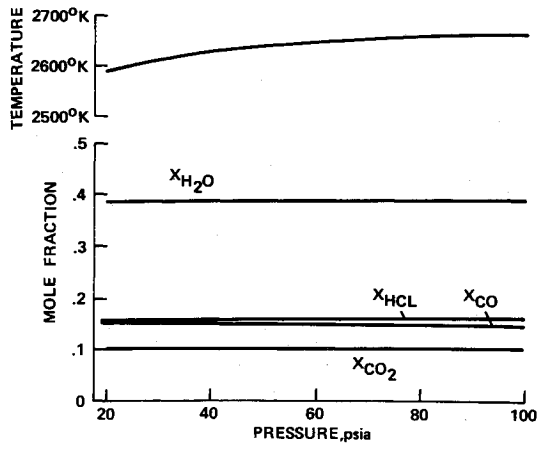

Fig. 4 Results of equilibrium calculation at 80 wt % AP in a polyurethane-AP propellant as a function of pressure.

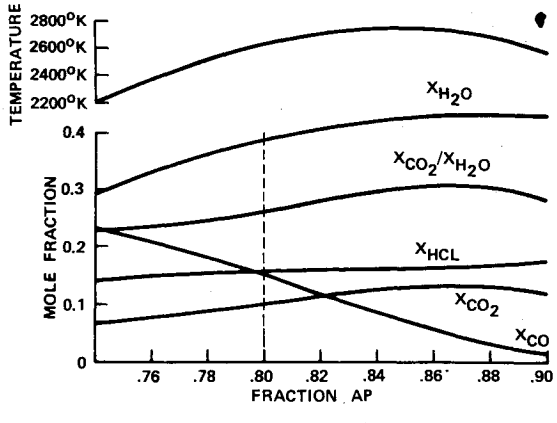

Fig. 5 Results of equilibrium calculation at 50 psia as a function of the fraction of total weight of a polyurethane-AP propellant given to AP.

† Obtained from the United States Air Force, Rocket Propulsion Laboratory, Edwards Air Force Base, and written by C. Selph, R. Hall, G. Cahill, and R. Patton.

§ The input values were those supplied by R. Reed, Thiokol Chemical Corp.

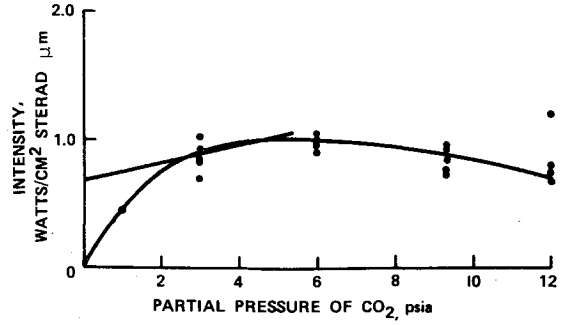

Fig. 6 Intensity of CO_2 emission at 4.3 μm as a function of partial pressure in a CO_2-argon mixture at 100 psia total pressure and 2600 °K; the straight line is the linear approximation used in the present study.

In order to assess the dependence of the intensity on partial pressure to account for the pressure pumping it was necessary to return to the intensity vs partial pressure plot obtained from the preliminary shock tube study.[15] Figure 6 is that plot for CO_2 gas at 2600°K. Over the pressure range of the present study this curve could be approximated by a straight line $I = I_0 + ap$ or more particularly $I = 0.66 + 0.077\ p$. Here p is the partial pressure of CO_2 and is taken to be 0.1 times the total pressure as predicted by the equilibrium calculation, over a wide range of pressures (Fig. 4) and a reasonable range of fuel to oxidizer ratios (Fig. 5). With this assumption the resultant adjusted intensity becomes

$$I_P = I[0.66 + 0.0077(P_N)]/[0.66 + 0.0077(P)] \quad (4)$$

As a result of this set of assumptions the fluctuations in the adjusted intensity correspond well to the anticipated fluctuations in concentration of the CO_2.

The critical nature of the pressure adjustment of the intensity must, however, be kept in mind in assessing the conclusions to be arrived at in this work.

Results

A large number of tests were conducted and reduced to quantitative data. These reduced tests displayed a whole spectrum of combustion behavior throughout which a few significant phenomena persisted in varying degrees of competition and coexistence with each other. In order to most clearly demonstrate the existence and significance of these phenomena a few tests have been selected for presentation. These are tests in which the phenomena are evident; not constituting "typical" tests, but rather points in the spectrum of behavior where circumstances permitted them to be easily seen. The phenomena observed included the oscillatory behavior associated with bulk mode instability in which the flushing time of the burner cavity coupled with the relaxation time of the thermal layer of the burning propellant or in which the propellant heterogeneity led to a "layer frequency" instability, the local intrinsic instability of the combustion itself, and the coupling of these two processes.

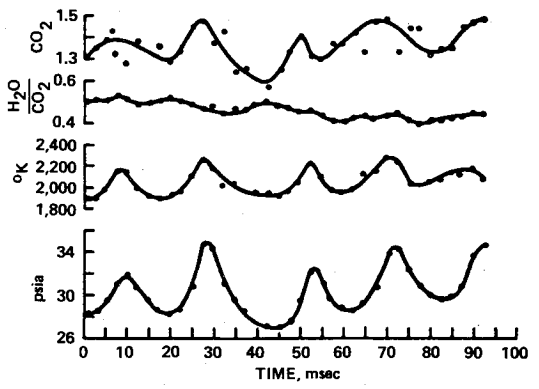

Fig.7 Example of bulk mode instability; temperature and composition fluctuate at the frequency of the pressure fluctuations; UCT propellant.

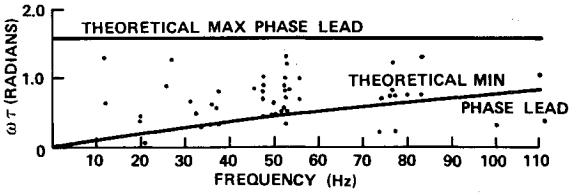

Fig. 8 Measured phase lead ($\omega\tau$) of mass efflux rate with respect to pressure vs frequency; phase is corrected to account for the time required for products to travel from the burning surface to the field of view. Theoretical prediction from Ref. 1.

Bulk Mode Instability

Bulk mode instability is taken here to refer to fluctuations in chamber conditions in which the flame temperature and composition are uniform in the plane parallel to the burning surface and are fluctuating at the same frequency as the pressure. Figure 7 is an example of the fluctuations observed under conditions of bulk mode instability. Note that the temperature and composition fluctuations, although at the same frequency as the pressure, are not in phase with the pressure, but consistently lead. In their theory of bulk mode instability, Price and Boggs[1] arrive at an expression from the perturbed mass balance of such a system which may be written in the form

$$\alpha = \omega \cot \omega\tau - (\Gamma/\beta\phi L^*) \quad (5)$$

where α is the exponential growth constant of the pressure oscillations from $P = \bar{P} + P_0 e^{\alpha t} \cos \omega t$, $\omega\tau$ is the phase lead of the mass rate with respect to the pressure, L^* is the characteristic length of the burner equal to the ratio of the free volume to the nozzle throat area, $\beta = \mu/\bar{C}_D R \bar{T}_g$ a constant (owing to the average values) equal to about 1.2×10^{-5} sec/cm, and Γ and ϕ are quantities whose values are both unity for the isothermal approximation and whose ratio is near unity for the isentropic case. Figure 8 is a plot of the mass rate lead measured (taken as the lead of the temperature and composition over pressure) vs frequency of pressure oscillation. Equation (5) predicts that during instability a phase lead, $0 < \omega\tau < \pi/2$ is always expected. Using estimated values of the parameters the theoretical minimum curve of Fig. 8 is determined at $\alpha = 0$, the stability limit,

Although the scatter of phase angles measured from cycle to cycle in a given test is considerable, owing both to the nature of the combustion processes and to the competition of the several phenomena, the trend is clear. The magnitude of the phase leads measured lie generally between the predicted theoretical minimum value calculation from Eq. (5) and the theoretical maximum of $\pi/2$ rad. No claim is made here for the precision of the predictions of the one-dimensional theory, quite the contrary. However, it seems appropriate to note that such simplified theories do have some predictive validity.

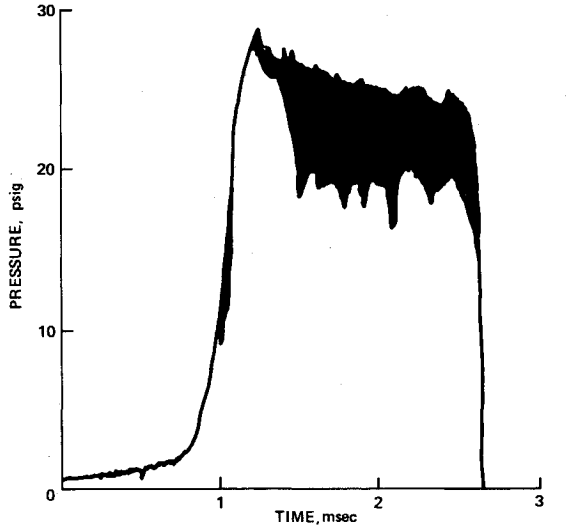

Fig. 9 Example of 2–3 Hz layer frequency superimposed on higher frequency oscillations; UCT propellant.

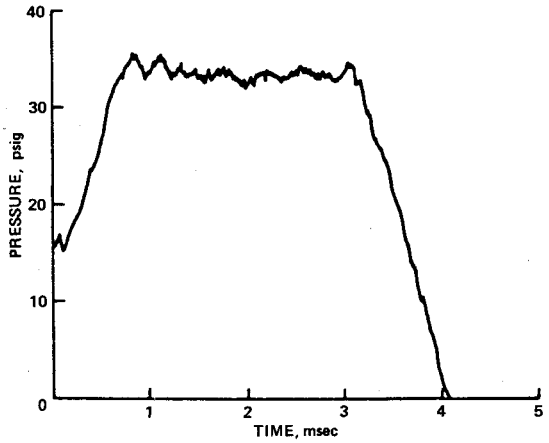

Fig. 10 Example of 2–3 Hz layer frequency during stable tests at large L^*, UCT propellant.

One attempt to explain deviations from predicted bulk mode instability behavior was made by Boggs and Beckstead.[12] They postulated a "layer frequency" concept based on observations of burning propellants, in which similarly sized AP particles become statistically phase correlated over the burning surface causing the pressure to oscillate with a frequency proportional to the burning rate divided by the particle diameter. In order to account for the fraction of the surface occupied by a particular sized particle at any given time they adjusted the r/D frequency by a factor, K_i, so that $f_i = K_i r/D_i$ where

$$K_i = \left\{ \frac{X_i}{\pi/6\,[\Sigma X_i + (\rho_{0x}/\rho_f)(1 - \Sigma X_i)]} \right\}^{1/3} \tag{6}$$

and i allows for the tendency of multimodal AP distributions to drive more than one frequency of oscillation. Table 1 shows the various expected frequencies and those observed (on the average) in the present tests. Clearly the results are only approximate. Note that the 600 μm AP which constitutes 55% of the propellant in each case is predicted to drive an oscillation of about 3 Hz. Figure 9 is a tracing of a pressure-time record which exhibits frequency components of very nearly 3 Hz. Even the mean pressure of stable tests (Fig. 10) contained this frequency. Such tests were not unusual, but initially caused considerable consternation since the oscillations appeared during tests at very large L^* which were expected to burn stably due to this large L^* value. The frequency was so low that it was always well below any other expected value and always was at approximately the same amplitude regardless of L^* value. It was also so low that at the scan rates of the spectrometric system employed it was not seen spectroscopically. The situation with respect to the fraction of the small AP particles is less straightforward. Recall that the frequency of the bulk mode instability was controlled by the particle size of the small particles. These are the values included in Table 1. As pointed out, these are not the exact frequencies

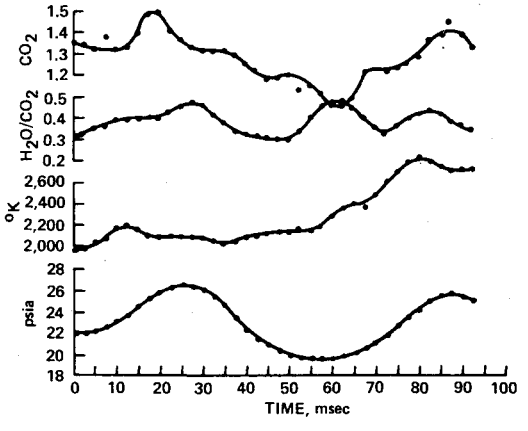

Fig. 11 Example of local intrinsic instability; temperature and composition fluctuate at a frequency different from that of the pressure fluctuation; UDO propellant.

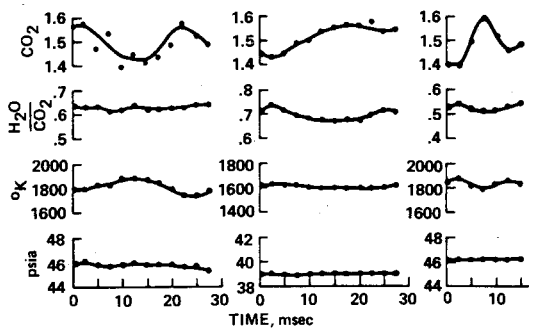

Fig. 12 Three examples of local intrinsic instability during stable tests at large values of L^*; UCT, UCD, and UDO propellants, respectively.

calculated, but the trend is clear; only the K_2 value is in need of adjustment. This is interesting in that the bulk mode behavior is reasonably well correlated by a mass balance theory in which the frequency is a parameter which is not predictable except through the burning rate. As indicated in Ref. 12 it is sometimes impossible to distinguish between the layer frequency and that predicted by 1-D theory. In practice, it appears the frequency is determined to large extent by the AP particle size which is not included in any theory except the layer frequency correlation. It is obvious that such a dependence of frequency on granularity cannot be universal since homogeneous propellants exhibit bulk mode instability also. Here, however, the distinction will not be made since aspects of both models are observed. The observation which is most significant is that the fluctuations in temperature and composition seen in these tests (500 to 600°K and 30 to 40%, respectively) are precisely what is predicted by thermochemical equilibrium considerations if the burning surface composition is fluctuating from 76% AP to 84% AP (see Fig. 5).

Local Intrinsic Instability

Local intrinsic instability refers to the situation where isolated, randomly phased regions on the burning surface of the propellant burn with a distinct periodicity unrelated to pressure or flow conditions. Such conditions might be related to AP particle size and certainly depend upon the propellant heterogeneity but are not taken here to include layer frequency instability. Figure 11 is a typical example of tests in which the temperature and composition fluctuated, while mutually at the same frequency, at a frequency different from, and uncorrelated to, the pressure fluctuations. If such fluctuations had occurred throughout the burner volume in a phase-correlated manner they would necessarily have had to have been reflected in the chamber pressure. They were not (see Ref. 16). For this reason it is concluded that such fluctuations were local and averaged to zero effect. In Fig. 12 are examples, rather surprising but not uncommon, of periodic local fluctuations in temperature and composition in what were otherwise extremely stable tests. It is interesting to note that in these tests as in that of Fig. 11 the temperature and composition appear to be 180° out of phase. Because of the flame density, the region immediately nearest to the spectrometer dominated. This resulted in a fictitious value of the absorptivity used in calculating the temperature. This is because the absorptivity is calculated by

$$\alpha = (I_s + I_E - I_{EA})/I_s \tag{7}$$

where I_s is the intensity of the radiation source with no combustion, I_E is the intensity of emission and I_{EA} is the intensity of the emission plus absorption during the combustion. When the intrinsic fluctuation results in a high I_E near the front edge, the absorptivity calculated is higher than the average absorptivity in the chamber. Then temperature calculated from

$$T = \frac{C_2}{\lambda} \Big/ \ln\left(1 + \frac{C_1}{\pi\lambda^5}\frac{\alpha}{I_E}\right) \tag{8}$$

is subsequently lower than it should be due to this high absorptivity value, and hence the fictitious 180° phase shift. This further emphasizes the local nature of these fluctuations.

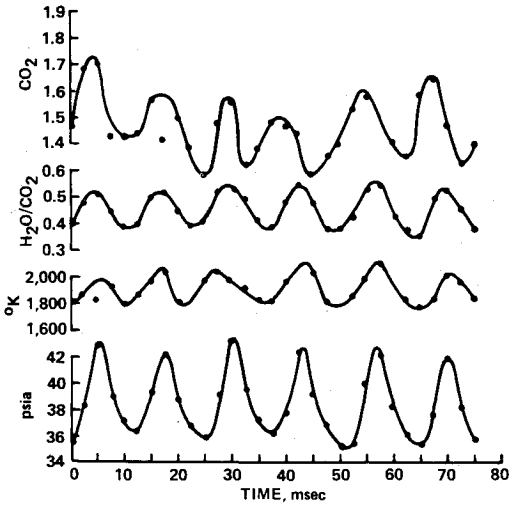

Fig. 13 Example of coupled bulk mode instability and intrinsic instability, UCT propellant.

The local intrinsic instability illustrated in Fig. 11 must have its origins in a mechanism other than one dependent on the AP particle size alone as was the case of the 3 Hz layer frequency discussed above and the dominant BMI frequency determined by the other AP fraction in each propellant. It must be noted that the frequency of the intrinsic instability observed was very nearly constant at about 60 to 80 Hz regardless of AP particle size. Whether it is due to local thermal explosions, sweeping off of a superheated surface layer, local composition fluctuations, or some other mechanism cannot be ascertained from the present work. The possibility that this is an artifact of the experiment is discussed and discounted in Ref. 15.

Coupled Bulk Mode and Intrinsic Instability

Under experimental conditions, in which the bulk mode instability frequency (which was dominated by AP particle size) and the intrinsic instability frequency (which was very nearly constant) were the same, a strong coupling was seen. Figure 13 is an example of this coupling of the two types of instability. These tests, unstable at about 80 Hz, exhibit large amplitude and strongly phase-locked oscillations in temperature and composition relative to the pressure while their phase lead with respect to pressure is maintained. The fictitious 180° phase shift between the composition and temperature that was explained in the case of the local intrinsic instability, no longer exists indicating that the fluctuations observed are once again representative of the entire field of view and not a local perturbation. This being so it is apparent that the formerly random local intrinsic fluctuations have now been phase-correlated by the bulk mode instability yielding the vigorous oscillations observed. Although the ratio of H_2O to CO_2 is of unknown significance it appears to serve as a gage of the severity of the instability. Note that in the coupled test shown the ratio now has large amplitude and is strongly correlated to the other fluctuations in the system in marked contrast to its behavior in either the bulk mode or local intrinsic instability tests.

Summary and Conclusions

The findings of this study include the observation of several types of instability: bulk mode, layer frequency, and local intrinsic instability. They include the observed tendency for these separate unstable combustion phenomena to influence and to couple with one another with the possible result of increased severity of instability.

In assessing these observations the assumption of gas phase equilibrium has been made. At the frequencies involved (10–100 Hz) such an assumption is almost always made, but here it has been experimentally tested. Within the resolution possible the temperature and composition fluctuations were in phase indicating that quasi-equilibrium was maintained. In the case of the local fluctuations in temperature and composition only local quasi-equilibrium can be claimed.

The observation of gas phase composition fluctuations implies by continuity that the instantaneous surface composition also fluctuated. This conclusion, which requires the equilibrium assumption just discussed, led to the attempt to correlate the observed temperature and composition fluctuations with the predictions resulting from allowing the surface composition to fluctuate. It was found that as little as ± 4 wt % fluctuation in AP content at the surface led to the 500°C and 40% CO_2 fluctuations observed in the gas phase of the bulk mode tests. This finding is extremely important since it demands the attention of the modelers of unstable combustion who have, up until the present, neglected consideration of composition fluctuations.

As a result of the present study it must be concluded that constant temperature and composition do not exist in a rocket chamber during unstable combustion, that quasi-equilibrium at frequencies below 100 Hz is probably a good assumption, and that constant surface composition does not exist for heterogeneous propellants during instability. In addition it should be clear that even for the apparently simple case of nonacoustic instability at low frequency there are a number of competing destabilizing processes simultaneously acting. Finally, it is clear that attempts to lump all low pressure, low frequency, nonacoustic instability into simple theories without recognizing this competitive and complementary situation is destined for less than total success.

References

[1] Price, E. W. and Boggs, T. L., "Nonacoustic Combustor Instability," TN 608-110, Naval Weapons Center (NWC), China Lake, Calif., to be published.

[2] Beckstead, M. W. and Price, E. W., "Nonacoustic Combustion Instability," *AIAA Journal*, Vol. 5, No. 11, Nov. 1967, pp. 1989-1996.

[3] Segal, R. and Strand, L., "A Theory of Low Frequency Combustion Instability in Solid Rocket Motors," *AIAA Journal*, Vol. 2, No. 4, April 1964, pp. 696–702.

[4] Wong, T. L., "*L** Instability," Ph. D. thesis, June 1969, Univ. of Utah, Salt Lake City, Utah.

[5] Culick, F. E. C., "A Review of Calculations for Unsteady Burning of a Solid Propellant," *AIAA Journal*, Vol. 6, No. 12, Dec. 1968, pp. 2241–2255.

[6] Price, E. W., "Relevance of Analytical Models for Perturbation of Combustion of Solid Propellants," *AIAA Journal*, Vol. 7, No. 1, Jan. 1969, pp. 153–154.

[7] Friedly, J. C. and Peterson, E. E., "Influence of Combustion Parameters on Instability in Solid Propellant Motors. Part II: Nonlinear Analysis," *AIAA Journal*, Vol. 4, No. 11, Nov. 1966, pp. 1932–1937.

[8] Brown, R. S. and Muzzy, R. J., "Linear and Nonlinear Pressure Coupled Combustion Instability of Solid Propellants," *AIAA Journal*, Vol. 8, No. 8, Aug. 1970, pp. 1492–1500.

[9] Krier, H., Summerfield, M., Mathes, H. B., and Price, E. W., "Entropy Waves Produced in Oscillatory Combustion of Solid Propellants," *AIAA Journal*, Vol. 7, No. 11, Nov. 1969, pp. 2079–2086.

[10] T'ien, J. S., Sirignano, W. A., and Summerfield, M., "Theory of *L** Instability with Temperature Oscillations," *AIAA Journal*, Vol. 8, No. 1, Jan. 1970, pp. 120–126.

[11] Schulz, E. M., "Propellant Flame Spectra During Depressurization," Ph.D. thesis, June 1970, Univ. of Utah, Salt Lake City, Utah.

[12] Boggs, T. L. and Beckstead, M. W., "Failure of Theories to Correlate Instability Data," *AIAA Journal*, Vol. 8, No. 4, April 1970, pp. 626–631.

[13] Herzberg, G., *Molecular Spectra and Molecular Structure. II. Infrared and Raman Spectra of Polyatomic Molecules*, Van Nostrand Princeton, N. J., 1945.

[14] Ferriso, C. C. and Ludwig, C. B., "High Temperature Spectral Emissivities of H_2O-CO_2 Mixtures in the 2.7 μ Region," *Applied Optics*, Vol. 3, No. 12, Dec. 1964, pp. 1435–1443.

[15] Eisel, J. L., "Flame Spectra of Solid Propellants During Unstable Combustion," Ph.D. thesis, June 1972, Univ. of Utah, Salt Lake City, Utah.

[16] Horton, M. D., Eisel, J. L. and Price, E. W., "Low Frequency Combustion Instability of Solid Rocket Propellants, Sept. 1962–1 May 1963," NOTS TP 3248, TPR 318, May 1963, U.S. Naval Ordnance Test Station, China Lake, Calif.